

Vibration modelling and structural modification of combine harvester thresher using operational modal analysis and finite element method

Hamed Ghafarzadeh Zare¹, Ali Maleki¹, Mohsen Irani Rahaghi^{*2} and Majid Lashgari³

¹Department of Mechanical Engineering of Biosystems, Shahrekord University, Iran

²Department of Mechanical Engineering, University of Kashan, Iran

³Department of Mechanical Engineering of Biosystems, Arak University, Iran

(Received January 13, 2019, Revised February 23, 2019, Accepted February 24, 2019)

Abstract. In present study, Operational Modal Analysis (OMA) was employed to carry out the dynamic and vibration analysis of the threshing unit of the combine harvester thresher as a mechanical component. The main study is to find the causes of vibration and to decrease it to enhance the lifetime and efficiency of the threshing unit. By utilizing OMA, structural modal parameters such as mode shapes, natural frequencies, and damping ratio was calculated. The combine harvester was excited by engine to vibrate different parts and accelerometer sensor collected acceleration signals at different speeds, and OMA was utilized by nonparametric and frequency analysis methods to obtain modal parameters while vibrating in real working conditions. Afterwards, finite element model was designed from the thresher and updated using the data obtained from the modal analysis. Using the conducted analyses, it was specified that proximity of the thresher pass frequency to one of the natural frequencies (16.64 Hz) was the most important effect of vibration in the thresher. Modification process of the structure was carried out by increasing mass required for changing the natural frequency location of the first mode to 12.4 Hz in order to reduce resonance and vibration of the thresher.

Keywords: structural modification; operational modal analysis; vibrations; thresher

1. Introduction

An important process in grain harvesting with combine harvester is threshing the materials using the thresher. An ideal thresher is one carries out complete threshing with maximum input crop and best grain separation while saves the shape and quality of the grain and minimizes grain loss Miu (2004). The distance between the threshing drum and the concave and the rotational speed of the threshing drum are among effective factors in design, performance, and failure of the threshing drum in a combine harvester. Vibration in the threshing drum causes the distance between the threshing drum and the concave to change, leading to an increase in threshing drum failure.

Vibrations of this unit cause the threshing action to fail and combine harvester loss to increase;

*Corresponding author, Ph.D., E-mail: irani@kashanu.ac.ir

therefore, it is highly important to study the vibration produced in the threshing unit. However, since measuring vibration in all working conditions on the farm is expensive, one of the ways to achieve the mentioned objectives is to use a vibration model by simulation methods in order to examine the effects of vibration on the machine's and the operator's performance. Using vibration modelling and dynamic analysis of the structure through mathematical model, finite element, and modal analysis, the causes and effects of vibration in different working conditions can be examined with minimum cost in Ewins (2000). Utilizing numerical approximation models such as finite element method to carry out dynamic analysis of complex large structures due to errors like those caused by using inappropriate hypotheses and theories, errors in modelling details of the structure, and unawareness about the characteristics of the materials, loading and different boundary conditions are associated with some problems. Therefore, modal test has been designed as a suitable tool to obtain the dynamic properties of structures. Experimental modal analysis methods are based on measuring the inputs and outputs, and extract the modal parameters of the structure by employing model identification methods such as peak picking, Ibrahim Time Domain (ITD) method, Complex Mode Indicator Function (CMIF), multidimensional modal method and so on by Cara (2016), Chandravanshi and Mukhopadhyay (2017), Ibrahim and Mikulcik (1997), De Oliveira (2018) and Li and Chen (2008). Experimental modal analysis is an appropriate method to extract natural frequencies and shape of modes, and verify the results of finite elements in the equipment in which measuring the excitation force is possible or the structure can be excited due to the small size of the equipment and the response can be recorded and the modal parameters of the structure can be extracted (Lim *et al.* 2009, Bim *et al.* 2012).

A large force is required to excite complex and large structures so that all shapes are excited in the mentioned frequency range. Using such a large force to excite the structure may cause destruction in the place of force exertion. On the other hand, this causes nonlinear behavior in the structure. In addition, existence of a lot of noise such as wind, vehicle traffic, and sound waves in the test environment causes problem to experimental modal analysis as is shown by Rahmatalla (2013), Hanson (2006) and Zhang (2014). These problems have caused researchers to propose new methods for modal analysis. In these methods, only the structure's response to environmental excitement is measured, and the modal parameters are determined without knowing the input exciting force. Therefore, these methods are known as ambient vibration analysis or operational modal analysis that were considered by Christof *et al.* (2010) and Mohanty and Rixen (2004).

Extracting dynamic properties of the structure using operational modal analysis is carried out by parametric and nonparametric methods. In parametric methods, a parametric model is matched for the system in the estimated time domain and directly measured for the responses obtained from the measuring data, while in nonparametric methods, by carrying out a set of mathematical operations on the measured data in the frequency domain, the dynamic properties of the structure are extracted by WENZEL and Pichler (2005), Zhang (2005) and Tarinejad and Damadipour (2014). One of the nonparametric methods is Frequency Domain Decomposition (FDD) which has some similarities with peak picking method and Complex Mode Indicator Function (CMIF). In this method that was first proposed by Brinker *et al.* (2001), power spectral density (PSD) matrix of the response is calculated and then singular value decomposition (SVD) method is applied on them, and it is used to obtain natural frequency values, damping coefficients, and the shape of the modes.

No studies have focused on vibration of thresher in combine harvester by operational modal analysis method yet. Therefore, due to the importance of the effect of the thresher's vibration on the combine harvester's performance, it seems necessary to examine the causes of vibration in the

thresher and fix it in order to reduce the combine loss.

The present study was aimed at carrying out dynamic analysis of combine harvester using operational modal analysis. Therefore, there was an attempt to use nonparametric method and frequency decomposition method in order to extract values of natural frequencies and damping coefficients, and the information obtained from the modal analysis was utilized to design and update the finite element model of the thresher. Afterwards, the vibration of the thresher was adjusted as much as possible by modifying the structure through weight modification method.

2. Operational modal analysis theory using Frequency Domain Decomposition (FDD) method

As observed in Eq. (1), the basis of the relations governing frequency domain decomposition method is based on the relationship between the inputs and outputs of a system (Brandt 2011).

$$G_{yy}(j\omega) = \overline{H}(j\omega)G_{xx}(j\omega)H^T(j\omega) \quad (1)$$

Where G_{xx} is input power spectral density matrix, G_{yy} is output power spectral density matrix, and $H(j\omega)$ is frequency response function matrix. For frequency response matrix, Eq. (2) can be written.

$$H(j\omega) = \sum_{k=1}^n \frac{Q_k}{j\omega - \lambda_k} + \frac{\overline{Q}}{j\omega - \lambda_k} \quad (2)$$

Where, Q_k indicates the remaining term, λ_k is the k^{th} natural frequency, the sign “-” indicates conjugate, and n represents the number of the given modes. Combining Eqs. (1) and (2), Eq. (3) for input and output power densities is obtained (Tarinejad and Damadipour 2014).

$$G_{yy}(j\omega) = \sum_{k=1}^n \left[\frac{Q_k}{j\omega - \lambda_k} + \frac{\overline{Q_k}}{j\omega - \lambda_k} \right] G_{xx}(j\omega) \left[\frac{Q_s}{j\omega - \lambda_s} + \frac{\overline{Q_s}}{j\omega - \lambda_s} \right] \quad (3)$$

If the input noise is white, power density matrix will be a matrix like $G_{xx}(j\omega) = C[I]$. By replacing this equation in Eq. (3) and simplifying it, Eq. (4) will be achieved.

$$G_{yy}(j\omega) = \sum_{k=1}^n \frac{A_k}{j\omega - \lambda_k} + \frac{\overline{A_k}}{j\omega - \lambda_k} + \frac{B_k}{-j\omega - \lambda_k} + \frac{\overline{B_k}}{-j\omega - \lambda_k} \quad (4)$$

Where A_k is the k^{th} remaining output power density, which is indicated as Eq. (5) (Brinker *et al.* 2001).

$$A_k = Q_k C \left(\sum_{s=1}^n \frac{\overline{Q_k}^T}{-\lambda_k - \lambda_s} + \frac{Q_k^T}{-\lambda_k - \lambda_s} \right) \quad (5)$$

Using the orthogonal property of the modes, the remaining will be as $A_k = Q_k C Q_k / 2\alpha_k$, where α_k is the k^{th} actual part of pole $\lambda_k = -\alpha_k + j\omega_k$. If the damping of the system is low, the remaining term will be appropriate with the mode shape and thus turns as $Q_k = 4\phi_k \gamma_k$ (See Eq. (6)) (Wenzel 2005).

$$A_k \propto Q_k C \overline{Q_k} = \phi_k \gamma_k C \gamma_k^T \phi_k^T = d_k Q_k Q_k^T \quad (6)$$

Where d_k is a scalar, ϕ_k is the vector of the k^{th} mode shape and γ_k is the vector of mode state. Finally, the response power density will be calculated based on the shape of the modes and the poles of the system as Eq. (7) (Brinker *et al.* 2001).

$$G_{yy}(j\omega) = \sum_{k=1}^n \left[\frac{d_k \phi_k \phi_k^T}{j\omega - \lambda_k} + \frac{\bar{d}_k \bar{\phi}_k \bar{\phi}_k^T}{j\omega - \bar{\lambda}_k} \right] \quad (7)$$

Eq. (7) states that a limited number of modes participate in creating the response in each frequency. If response power spectral density matrix in each frequency is decomposed into its values and singular vectors, since there is a direct relationship between singular values and the participation coefficient of the modes, the number of non-zero singular values indicates the number of modes that creates the system's response in that frequency, and the peaks of the system's first singular values will be equal to the natural frequencies of the system. On the other hand, singular vectors corresponding the first peaks of the singular values estimate the system's mode shape vectors. In Eq. (8), U_i and S_i are the system's singular values matrix in frequency ω_i (Brinker *et al.* 2001).

$$G_{yy}(j\omega_i) = U_i S_i U_i^H \quad (8)$$

After the power spectral density function is determined, it will return to time domain by carrying out inverse Fourier transform, which is called correlation function of a degree of freedom. The system's damping is estimated from the decline rate of this function in time domain (Magalhaes *et al.* 2008), such that first all values of the function at its extremums are found that are shown as r_k , then logarithmic decrement δ was calculated through Eq. (9).

$$\delta = \frac{2}{k} \text{Ln} \left(\frac{r_0}{|r_k|} \right) \quad (9)$$

Where r_0 is the initial of the correlation function and r_k is the final value of the k^{th} . Therefore, the logarithmic decrement and the initial value of the correlation function can be calculated from a linear regression on δk and $2\ln(r_k)$ (Brewick 2013).

$$2\ln(r_k) = 2\ln(r_0) - \delta k \quad (10)$$

Thus, damping ratio is determined using Eq. (11).

$$\zeta = \frac{\delta}{\sqrt{\delta^2 + 4\pi^2}} \quad (11)$$

3. Experimental procedure and results

3.1 Operational modal test

To measure the vibration of the thresher in practical conditions, a piezoelectric accelerometer sensor DYTRAN/MODEL3255A2 (100 mV/g sensitivity, 50g range, 10 grams, -60 to +250°F

Operation) and an analyzer device and a signal processing software MScopeVES were employed. In order to carry out the analysis, the combine harvester was started in its normal conditions and all parts were set in operation. The pulse system was regulated for sampling interval of 1.953 ms. Therefore, about 6,144 data points were acquired, corresponding to a measurement time of 12s.

Due to the geometry of the structure, 4 points were chosen on the bearings of the threshing drum. Measuring for each speed was carried out in three phases. In each phase, a sensor measured the vibrations of a new point of the structure, and another sensor was considered as the reference sensor. The measured points on the bearings are indicated in Fig. 1.

Fig. 2 presents a sample signal related to the threshing drum in horizontal and vertical positions. As seen, the domain of the signals in vertical position is more than the horizontal position; therefore, it can be concluded that the threshing drum receives more vibration in vertical position compared to the horizontal position.

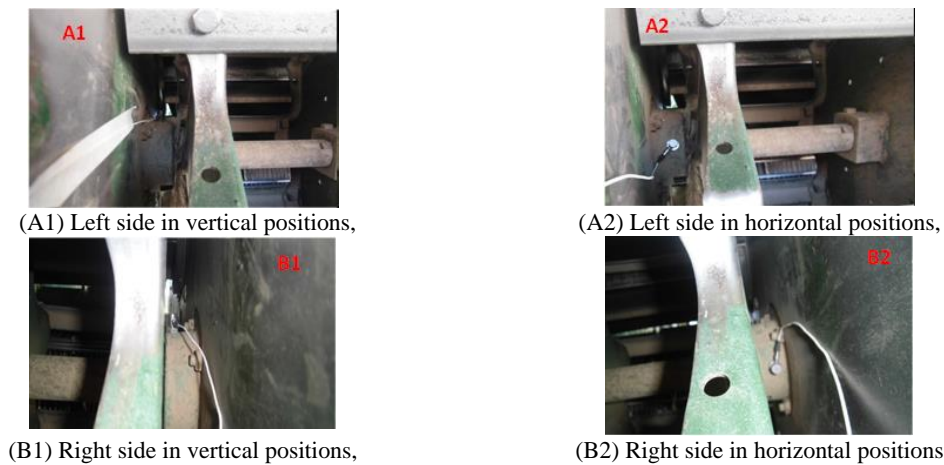


Fig. 1 The location of the sensors on the bearings of the thresher in horizontal and vertical positions

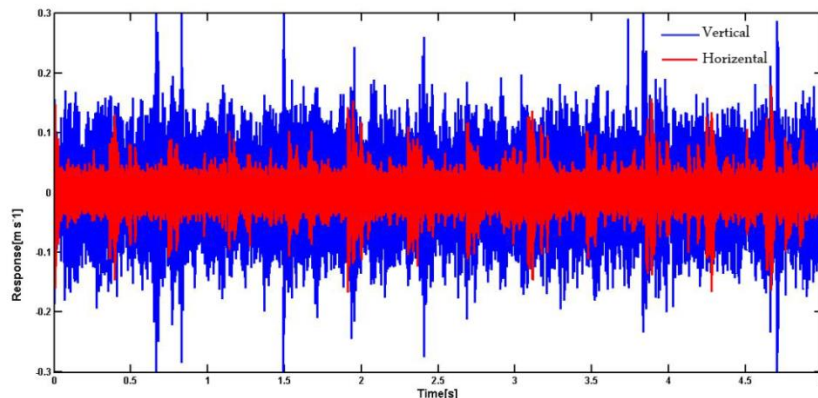


Fig. 2 Vertical and Horizontal vibration signals

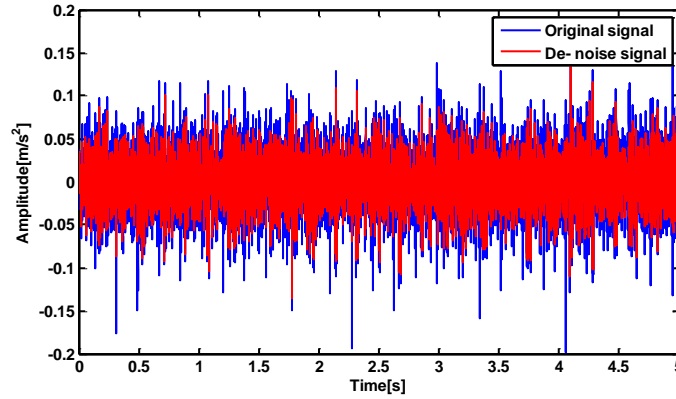


Fig. 3 Original and de-noised vibration signals

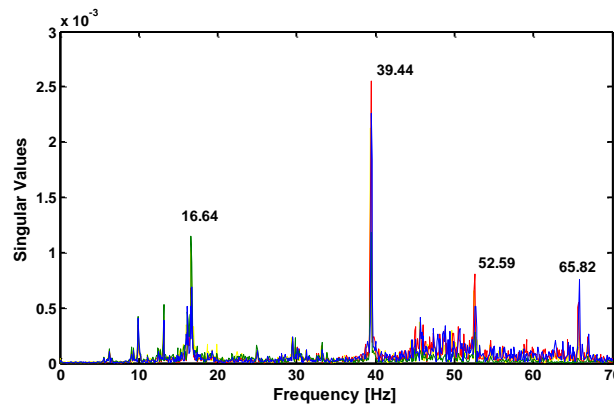


Fig. 4 Singular values of the PSD matrix of the response

While measuring vibration signals, some disturbing factors come up and distort the results. Some of these factors include shocks and sudden changes in speed or load, which are frequently observed in agricultural machinery. However, the quality of operational modal analysis depends on the quality of the response data; therefore, a wavelet de-noising was used to reduce the effect of noise on the recorded data. As a result, the time signals were fed into MATLAB, and the wavelet de-noising `coif2` level 3 that is used for vibration signals with high accuracy was employed to reduce the effect of noise on the signals. For pattern recognition of specific data series, universal threshold rule as indicated in Eq. (12) was used, where N is the signal length and σ is noise standard deviation (Misiti *et al.* 2008, Donoho 1995, Moosavian *et al.* 2015). In Fig. 3, a sample of the thresher's vibration signal and de-noising signal is presented with the help of wavelet function.

$$t = \sigma \sqrt{2 \log N} \quad (12)$$

Afterwards, de-noising signals used in MATLAB were utilized to calculate the response power spectral matrix, and singular values decomposition method was applied on it. Finally, by drawing each singular value, resonance peaks of the system were determined with respect to different

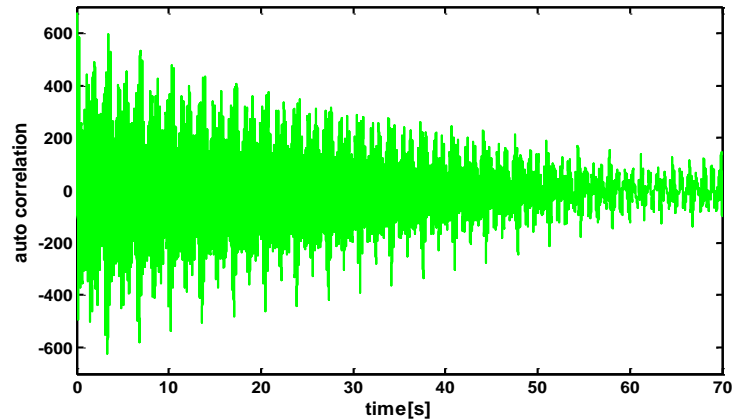


Fig. 5 Auto correlation functions associated with modes 1

frequencies, and the system's damping was estimated using Eq. (11). Fig. 4 presents singular values of power spectral density matrix based on different frequencies. Since during the measurement, the only vibration source was the combine's engine and powertrain, the diagram indicates that the first four modes of the structure are obviously excited. Fig. 5 presents the auto-correlation function calculated from the power spectral density function of the first mode. Damping coefficients are determined by measuring the extreme points in Fig. 5 and using Eqs. (10) and (11).

3.2 Finite element modeling of the thresher

In order to carry out geometric modelling and simulation of the thresher by finite element method, ABAQUS finite element software was employed. First, the primary geometric model was designed in ABAQUS software. In modelling the thresher, four parts of the thresher including 8 blades, 4 plates, rotors, and bearings were made. These parts were all solid-type and defined flexible. Design properties included shape, thickness, size, and the angles of the components of the thresher, which were designed according to John Deere 955 combine harvester. In materials definition section in the software, steel with elastic modulus of 200 GPa, density of 7800 kg/m³, and Poisson's Ratio 0.3 were defined. In the assembly environment, the four components of the thresher were elicited, and in the module of "Interaction" between surfaces of the parts that are in touch with one another, "Tie" was applied (See Fig. 6). Afterwards, meshing the thresher was carried out as first-order four-node quadrilateral elements. Since the accuracy of the analysis outputs depends on the size of the elements, gradation of the elements decreased and increased regularly in order to homogenize the solution, and the effect of these change on the output results was examined and the best size of the elements was selected for the meshing (See Fig. 6). In the process of solution by selecting frequency analysis, the natural frequencies of the system were extracted. In Fig. 7, first to fourth mode shapes of the thresher obtained from ABAQUS software are observed.

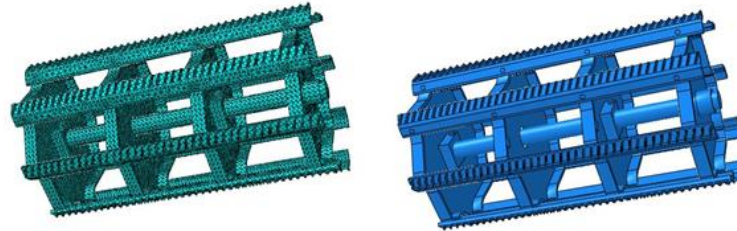


Fig. 6 The assembled and meshed model of the thresher

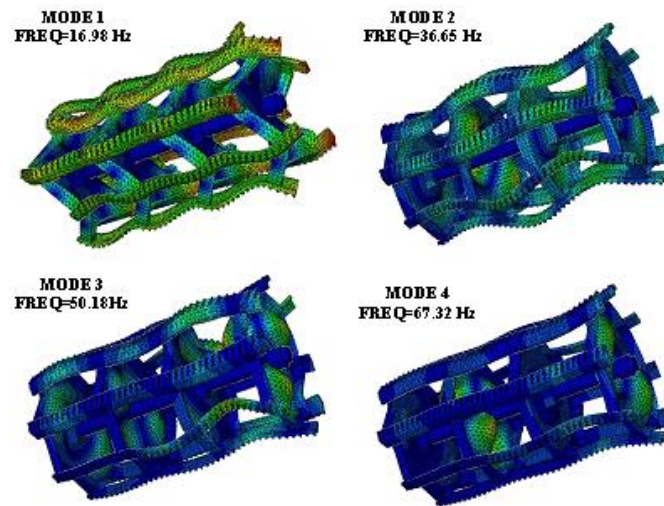


Fig. 7 The first 4 mode shapes of combine harvester thresher calculated by finite element model

3.3 Investigating the effect of the threshing's rotation speed on the system's critical speeds

From the operator's cabin, the rotational speed of the threshing drum can be adjusted from 750 to 1500 rpm. While harvesting barley and wheat, the rotational speed of the threshing drum is usually adjusted between 900 and 1200 rpm depending on the material density and crop moisture. In order to examine the effect of the threshing's rotation speed on the thresher's natural frequencies, the signals were measured in four common speeds of the threshing 750, 1000, 1200, and 1500 rpm with 5 replicates, and a number of signal indications including root mean square, energy, and entropy were extracted according to the equations presented in Table 1. The results presented in Table 2 indicate that root mean square, energy, and entropy were significantly higher in speed 1000 rpm compared to other speeds. Frequency analysis method was employed to determine the natural frequencies of the thresher, and the results are presented in Table 3. Afterwards, Campbell diagram (See Fig. 8) was drawn for different speeds, where the intersection of the excitation line and the line related to the natural frequencies indicates the critical speed in the system.

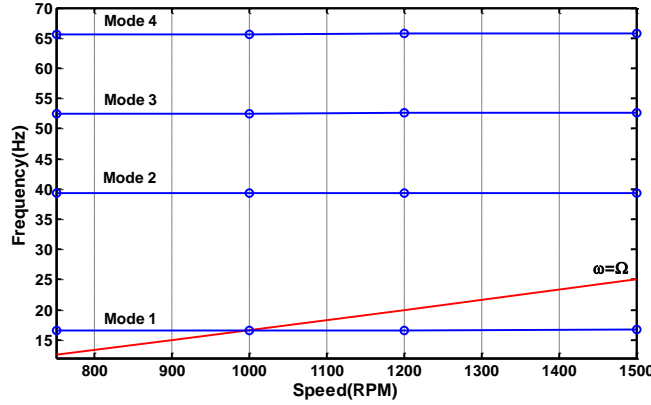


Fig. 8 Campbell plot Red line: bisector of the first quadrant ($\Omega=\omega$)

Table 1 The parameters extracted from the signals

Function	Equation
RMS*	$F_1 = \sqrt{\frac{\sum_{n=1}^N (x(n))^2}{N}}$
Energy	$F_2 = \sum_{n=1}^N (x(n))^2$
Entropy	$F_3 = \sum_{n=1}^N (x(n)) * \log\left(\frac{1}{x(n)}\right)^2$

* $x(n)$ is a signal series for $n = 1, 2, \dots, N$, N is the number of data points

Table 2 The values extracted from the signals

Speed(rpm)	RMS	Energy(j)	Entropy(j/k)
750	0.0196	84.7851	2.4461
1000	0.297	193.6902	2.8183
1200	0.0213	99.7406	2.4943
1500	0.0204	91.1437	2.4765

According to Fig. 8, it can be seen that the thresher at speed 1000 rpm has a critical speed; therefore, the values obtained for root mean square, energy, and entropy at speed 1000 rpm are confirmed.

Table 3 FEM results and OMA results under different rotating speeds

Speed(rpm)	f1(Hz)	ξ_1	f2(Hz)	ξ_2	f3(Hz)	ξ_3	f4(Hz)	ξ_4
750	16.64	0.361	39.35	0.140	52.49	0.086	65.64	0.059
1000	16.64	0.323	39.35	0.183	52.49	0.079	65.64	0.042
1200	16.73	0.294	39.44	0.128	52.59	0.068	65.73	0.038
1500	16.64	0.391	39.44	0.109	52.59	0.071	65.82	0.047

3.4 Validation of the finite element results by experimental test

In order to compare the analytical and experimental results of Natural Frequency Difference (NFD) value, the predicted and measured natural frequencies were calculated using Eq. (13), and its 3-dimensional diagram was drawn (See Fig. 9). Many researchers have utilized NFD to compare the values of measured and calculated frequencies (Khatibi *et al.* 2012, Rovenscek 2014). The advantage of this method is that the difference of the natural frequencies among all possible combinations from the members of the two frequency sets of experimental and analytical model can easily be assessed (Ewins 2000). The importance of this issue will be clear when there is no one-to-one correspondence between the four measured and predicted natural frequencies, or in other words, when some modes of the structure (usually close modes) cannot be extracted using the measured responses and the applied algorithms. Small NFD values in diagonal positions and large NFD values in non-diagonal positions indicate that there is a high compatibility between the analytical and test results.

$$NFD_{i,j} = \frac{|\omega_i - \omega_j|}{\min(\omega_i, \omega_j)} \quad (13)$$

Where ω_i and ω_j are the natural frequencies obtained from finite element model and operational model analysis, respectively. In Table 4, the natural frequencies obtained from the theoretical results and the mean values obtained from the test in different speeds of the thresher and the percentage errors are presented.

Table 4 Natural frequencies obtained from the theoretical results and the test and percentage error

Mode No.	1	2	3	4
FEM (Hz)	16.98	36.65	50.18	67.32
FDD (Hz)	16.66	39.39	52.54	65.71
Error (%)	1.90	7.49	4.70	2.45

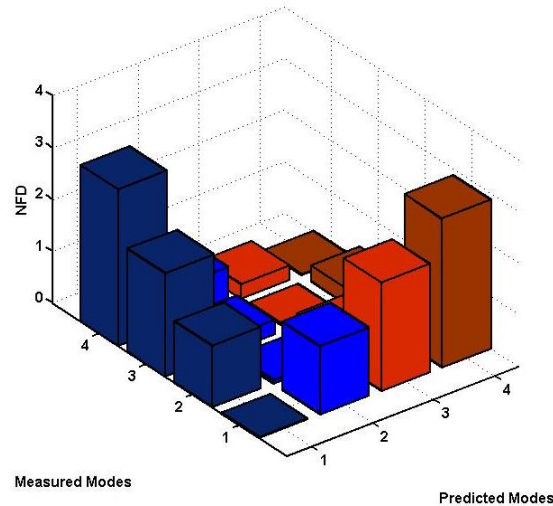


Fig. 9 Natural Frequency Difference (NFD) diagram

3.5 Structural modification

Modifying the structure as one of the applications of modal analysis is a technique to consider the effect of physical parameters of a structure on its dynamic properties, i.e., natural frequencies and mode shape in order to improve the structure's dynamic behavior (Park 2000). For this purpose, it is necessary to create an accurate model of the structure in order to be able to calculate the effect of the modifications on the structure. The proximity of the thresher's excitation frequency to its natural frequency in speed 1000 rpm in the first mode (16.64 Hz) causes large vibrations in the structure. In order to reduce the magnitude of vibrations, natural frequencies should be in an enough distance from the excitation frequency. In the present study; therefore, modification of the threshing unit was aimed at decreasing its vibrations by changing the natural frequency. Due to its complexity, the process of modifying the structure can be carried out by changing the mass and hardness (Ziaei 1997, Kyprianou *et al.* 2005). As presented in the study, modification of the structure was conducted by changing the mass on the finite element model. Since the masses placed on the maximum and minimum points of the mode shapes lead to more frequency changes compared to node points, so these points are the best position of the masses in order to modify the natural frequencies. The process of modifying the structure was carried out by adding the point mass in different parts of the structure, and it was concluded that applying 4 point masses of 62 gram in the parts determined in Fig. 10 led to a change in natural frequency of the thresher from 16.98 to 12.4 Hz in the first mode.

In Table 5, the natural frequencies of the system in the first four modes before and after modifying the structure. According to the rotational speed of the threshing drum for wheat which is normally between 900 and 1200 rpm, and given the natural frequency value in the first four modes after modifying the structure, it can be concluded that the threshing drum does not experience resonance phenomenon in this working interval.

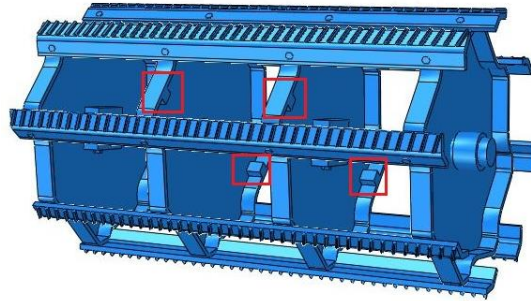


Fig. 10 the locations of applying mass in order to structural modification



Fig. 11 the locations of applying mass on the thresher

Table 4 the first four modes before and after modifying the structure

Mode No.	1	2	3	4
The first four modes before modifying the structure	16.98	36.65	50.18	67.32
The first four modes after modifying the structure	12.4	30.45	42.81	55.09
Error (%)	37%	20%	17%	22%

As observed in the Fig. 11, after the structure was modified on the model and the appropriate place to install the masses was selected, the changes were applied on the thresher in the real environment. Afterwards, operational modal analysis was carried out on the modified thresher. After the data were analyzed, it was concluded that the natural frequency of the thresher in the first mode in the modified thresher was with a mass of 13.2 Hz, which showed an error of below 7% compared to the results of the finite element model. Therefore, it can be assured that using these two methods of modification, the thresher will not undergo the phenomenon of resonance.

4. Conclusions

The purpose of this study is to determine vibration characteristics and present a vibration model of the thresher. The vibration responses of the thresher were recorded in working conditions on the bearings of the thresher. After the signals were de-noised, the primary data were analyzed and the reliability of the data was assured. Finally it was determined that the measurement conditions were almost the same for each phase and the measurements had an almost acceptable reliability. Afterwards, frequency domain decomposition technique was used to extract natural frequencies and system's damping ratios, then the thresher's finite element model was constructed using ABAQUS software and the frequencies were analyzed. Comparing the obtained results of finite element modeling to operational modal analysis, this model was updated with an acceptable accuracy. After updating the finite element model, it can be used in subsequent analyses such as predicting the response to a force applied on the structure, stress analysis, and etc.

- To evaluate the effect of the thresher's rotation speed and the feeding rate of the materials between the threshing drum and concave on natural frequencies, modal analysis was carried out in different speeds of the thresher and different feeding rate of materials per thresher unit. It was determined that these factors had no significant effect on the system's natural frequencies. Therefore, the thresher's natural frequency is not influenced by the feeding rate of the materials; rather it depends on mass, hardness, and the support type.
- Investigating signal parameters in different speeds of the thresher, it was specified that these parameters had significantly higher values in rotation speed of 1000 rpm compared to other speeds.
- By examining the range of the natural and excitation frequencies of the threshing unit and also considering the diagram obtained from decomposing the singular values of the power spectral density matrix and Campbell diagram, a resonance frequency was found for the given structure, which is the major cause of vibration in the thresher. Moreover, speed 1000 rpm was determined as the critical speed of the thresher.
- In order to reduce the level of vibrations, the thresher's excitation frequency should be far enough from the natural frequency; therefore, the process of modifying the structure is carried out by changing the mass applied on the finite element model, and the changes were applied on the thresher in the real environment.

References

- Bing, B., Zhang, L., Guo, T. and Liu, C. (2012), "Analysis of dynamic characteristics of the main shaft system in a hydro-turbine based on ansys", *J. Procedia Eng.*, **31**, 654-658.
- Brandt, A. (2011), *Noise and Vibration Analysis: Signal Analysis and Experimental Procedures*. 1st Ed., John Wiley & Sons.
- Brewick, P. and Smyth, A. (2013), "An investigation of the effects of traffic induced local dynamics on global damping estimates using operational modal analysis", *Mech. Syst. Signal Pr.*, **41**, 433-453.
- Brincker, R., Zhang, L. and Andersen, P. (2001), "Modal identification of output only systems using frequency domain decomposition", *Smart Mater. Struct.*, **10**, 441- 445.
- Cara, J. (2016), "Computing the modal mass from the state space model in combined experimental – operational modal analysis", *J. Sound Vib.*, **370**, 94-110.
- Chandravanshi, M.L. and Mukhopadhyay, A.K. (2017), "Analysis of variations in vibration behavior of vibratory feeder due to change in stiffness of helical springs using FEM and EMA methods", *J. Braz. Soc.*

- Mech. Sci. Eng.*, **39**, 3343-3362.
- Christof, D., Gert, D. and Patrick, G. (2010), "An operational modal analysis approach based on parametrically identified multivariable transmissibilities", *Mech. Syst. Signal Pr.*, **24**, 1250-1259.
- Deoliveira, F.M.V.M., Ipina, J.E.P. and Bavastri C.A. (2018), "Experimental identification of structural changes and cracks in beams using a single accelerometer", *J. Braz. Soc. Mech. Sci. Eng.*, **40**(106).
- Donoho, D.L. (1995), "De-noising by Soft-thresholding", *IEEE T. Inform. Theory*, 613-627.
- Ewins, D.J. (2000), *Modal Testing: Theory Practice and Application*, Research Studies Press Ltd. England.
- Hanson, D. (2006), *Operational Modal Analysis and Model Updating with a Cyclostationary Input*, PhD Thesis, University of New South Wales, Australia.
- Ibrahim, S.R. and Mikulcik, E.C. (1997), "A method for the direct identification of vibration parameters from the free response", *Shock Vib. Bulletin*, **47**, 183-198.
- Khatibi, M.M., Ashory, M.R., Malekjafarian, A. and Brincker, R. (2012), "Mass-stiffness change method for scaling of operational mode shapes", *Mech. Syst. Signal Pr.*, **26**, 34-59.
- Kyprianou, A., Mottershead, J.E. and Ouyang, H. (2005), "Structural modification. Part 2: assignment of natural frequencies and antiresonances by an added beam", *J. Sound Vib.*, **284**, 267-281.
- Li, X. and Chen, L.T. (2008), "Modal analysis of coupled vibration of belt drive systems", *Appl. Math. Mech. - Engl.*, **29**, 9-13.
- Lim, H., Chung, J. and Yoo, H. (2009), "Modal analysis of a rotating multi-packet blade system", *J. Sound Vib.*, **325**, 513-531.
- Magalhaes, F., Caetano, E. and Cunha, A. (2008), "Operational modal analysis and finite element model correlation of the Braga Stadium suspended roof", *Eng. Struct.*, **30**, 1688-1698.
- Misiti, M., Misiti, Y., Oppenheim, G. and Poggi, J. (2008), *Matlab user's guide: wavelet toolbox™ 4*. Natick (Mass): The Math Works Inc.
- Miu, P.I. (2004), "Mathematical modeling of material other than grain separation in threshing units", *ASAE Meeting Presentation, ASAE Paper No. 993208. ASAE, St. Joseph, MI, USA*.
- Mohanty, P. and Rixen, D.J. (2004), "A modified Ibrahim time domain algorithm for operational modal analysis including harmonic excitation", *J. Sound Vib.*, **275**, 375-390.
- Moosavian, A., Khazaei, M., Najafi, G.H., Kettner, M. and Mamat, R. (2015), "Spark plug fault recognition based on sensor fusion and classifier combination using Dempster-Shafer evidence theory", *Appl. Acoust.*, **93**, 120-129.
- Park, Y.H. and Park, Y.S. (2000), "Structural modification based on measured frequency response function: an exact eigenproperties reallocation", *J. Sound Vib.*, **237**, 411-426.
- Rahmatalla, S., Hudson, K. and Liu, Y. (2013), "Finite element modal analysis and vibration-waveforms in health inspection of old bridges", *J. Finite Elem. Anal. Des.*, **78**, 40-46.
- Rovscek D., Slavic J. and Boltezar M. (2014), "Operational mode-shape normalisation with a structural modification for small and light structures", *Mech. Syst. Signal Pr.*, **42**, 1-13
- Tarinejad, R. and Damadipour, M. (2014), "Modal identification of structures by a novel approach based on FDD-wavelet method", *J. Sound Vib.*, **333**, 1024-1045.
- Wenzel, H. and Pichler, D. (2005), *Ambient Vibration Monitoring*. 1st Ed., John Wiley & Sons.
- Zhang, G., Ma, J., Chen, Z. and Wang, R. (2014), "Automated eigensystem realization algorithm for operational modal analysis", *J. Sound Vib.*, **333**, 3550-3563.
- Zhang, L., Brincker, R. and Andersen, R. (2005), "An overview of operational modal analysis major development and issues", *Proceedings of the 1st International Operational Modal Analysis Conference (IOMAC)*, Copenhagen Denmark, 262-269.
- Ziaeirad, S. (1997), *Methods for Updating Numerical Models in Structural Dynamic*, PhD Thesis, Imperial College London.